ISSN 1392–1320 MATERIALS SCIENCE (MEDŽIAGOTYRA). Vol. 16, No. 1. 2010

Synthesis of Gadolinium Doped Ceria Solid Electrolyte by Solid State Reactions of CeO_2/Gd_2O_3 Multilayer Thin Films

Saulius BURINSKAS[1*], Vytautas ADOMONIS[1], Virūnas ŽALNIERUKYNAS[1], Julius DUDONIS[1], Darius MILČIUS[2]

[1]*Department of Physics, Kaunas University of Technology, Studentų 50, LT-51368, Kaunas, Lithuania*
[2]*Lithuania Energy Institute, Breslaujos 3, LT-44403 Kaunas, Lithuania*

Received 16 September 2009; accepted 05 March 2010

The purpose of the present investigation is to study formation of Gd doped CeO_2 solid electrolyte thin films by solid state reactions of CeO_2/Gd_2O_3 multilayer thin films deposited by reactive magnetron sputtering. Synthesis of cerium and gadolinium oxide layers on Si and glass substrates was made by sputtering metallic Ce and Gd targets in $Ar + O_2$ atmosphere. Single layer thickness was kept at 42 nm for CeO_2 and 5 nm for Gd_2O_3. Mixing of the layers and formation of $Gd_{0.1}Ce_{0.80}O_{1.90}$ (GDC10) during annealing of coatings in 450 °C – 650 °C temperatures took place. X-ray diffraction (XRD) studies using monochromatic CuK_α radiation showed XRD (111) and (220) peaks shifting and asymmetry changes after sample annealing. The annealing related crystallite size growth was confirmed using Scherrer equation and Williamson-Hall plot. The investigation of morphology of the layers with a scanning electron microscope (SEM) showed no multilayer structure in the films. Optical characterization of thin films on glass substrate was made by UV-VIS spectrophotometer. Energy band gaps of undoped and Gd doped CeO_2 films were determined using Tauc's relationship and were found to be 3.08 eV and 3.13 eV respectively.
Keywords: CeO2, Gd2O3, multilayer, reactive, magnetron, sputtering, solid electrolyte, SOFC.

INTRODUCTION

Thin films of gadolinium doped cerium oxide (GDC) are intensively investigated for an application as a solid electrolyte in solid oxide fuel cells (SOFC) [1]. The higher ionic conductivity of doped ceria comparing it to the conventional electrolyte material of yttria-stabilized zirconia (YSZ) at intermediate temperatures (500 °C – 700 °C) makes it very attractive material, because lower operation temperature allows to use cheaper SOFC components, to overcome fast ageing and other problems [2, 3]. The main problem of most conventional mechanical methods such as screen printing, tape casting or dry pressing is inability to form dense solid electrolyte layer on porous anode substrate [3]. Also usage of thick film electrolyte does not ensure sufficient ionic conductivity in intermediate temperatures [2]. Therefore many authors are using more sophisticated physical vapour deposition (PVD) technologies, such as reactive DC magnetron sputtering [2], plasma assisted electron beam evaporation [4], pulsed layer deposition [5], aerosol-assisted metalo-organic vapour deposition (MOCVD) [6] and others for deposition of thin film electrolyte coatings. Reactive DC magnetron sputtering is widely used for deposition of dense metal oxide coatings despite some of its drawbacks like discharge hysteresis and non-stoichiometric oxide formation in metallic sputtering mode and low deposition speed in oxide sputtering mode [7]. Solid state reactions are widely used to dope various materials and also it was demonstrated that this method is suitable for Gd doped ceria formation [8]. But in such method higher than 1000 °C temperatures are used to ensure fast diffusion. Solid state reaction during annealing of reactive DC magnetron deposited CeO_2/Gd_2O_3 multilayer coatings was never chosen for formation of Gd doped ceria. When the outer ring of magnets in magnetron is strengthened relative to the central pole (type-1 unbalanced magnetron), not all the field lines are closed between the central and outer poles in the magnetron, but some are directed towards the substrate, what causes substrate bombardment by ions. Ion current densities can reach 5 mA/cm^2 and greater values. As a result, unlike in other ion-plating processes, the ion-to-atom arrival ratio at the substrate remains constant with increasing deposition rate, that helps to achieve dense film structure. [9] Since magnetron deposited thin films may include many point defects due to ion bombardment from plasma during film growth, enhanced diffusion and fast mixing of deposited multilayer is expected at intermediate temperatures range from 450 °C to 650 °C.

Various amount of Gd doping was used for formation of ceria solid electrolyte. While $Gd_{0.1}Ce_{0.90}O_{1.95}$ (often abbreviated as GDC10) has the highest lattice conductivity, $Gd_{0.2}Ce_{0.80}O_{1.90}$ (GDC20) has higher total conductivity because its grain boundary contribution seems to be more tolerant of impurities [10]. But experiments have shown that GDC10 is more resistant to reduction from Ce^{4+} to Ce^{3+} than GDC20 [1], so GDC10 composition seems to be the best choice for the synthesis of solid electrolyte.

There is not enough information about possibility to form GDC electrolyte by solid state reactions of CeO_2/Gd_2O_3 multilayer thin films, therefore, the goal of the present investigation is to analyze morphology, microstructure and optical properties of as deposited and annealed CeO_2/Gd_2O_3 multilayer thin films deposited by reactive direct current magnetron sputtering.

[*]Corresponding author. Tel.: +370-687-75560; fax: +370-37-456472.
E-mail address: *saulius.burinskas@stud.ktu.lt* (S. Burinskas)

EXPERIMENTAL PROCEDURE

Multilayer CeO_2/Gd_2O_3 thin films were deposited by direct current unbalanced magnetron sputtering on the room-temperature Si substrates. Discharge was made in an argon and oxygen atmosphere. Before the deposition, the surface of the substrates was ultrasonically cleaned in pure acetone for organic contaminants and in pure ethanol for inorganic contaminants. A vacuum chamber was evacuated to the pressure of $5.0 \cdot 10^{-3}$ Pa. Working pressure was kept constant at $2.7 \cdot 10^{-1}$ Pa by adjusting argon gas flow with mechanical gas inlet. Oxygen flow was kept constant at 20 sccm (standard cm^3/min) with electronic gas flow regulator Aalborg GFC17. Substrate holder was moved at 6 cm distance over the target. Deposition was performed with a constant discharge current density of 39 mA/cm^2 for Ce and 24 mA/cm^2 for Gd cathode. Since cathodes were cooled indirectly using copper backing plate to avoid reaction of Ce and Gd with water, cathode temperature was higher than that of conventional magnetron systems and oxygen thermal desorption allowed us to operate in half-metallic sputtering mode reaching high deposition speeds. The deposition speed was measured with precise weighting method to be 1.3 nm/s CeO_2 for and 1.0 nm/s for Gd_2O_3. The thickness of single layer was 39.0 nm (30 s deposition time) for CeO_2 and 6 nm (6 s deposition time) for Gd_2O_3. Total coating thickness was expected to be 450 nm (10 bilayers). Different timing was calculated to achieve 10w% Gd doping level.

The crystallographic structure of thin films was investigated by X-ray diffraction (XRD) studies using Bruker D8 Discover diffractometer with monochromatic $Cu_{K\alpha}$ radiation ($\lambda = 0.15418$ nm). Scherrer equation (using full width at half maximum of XRD peaks β) and Williamson-Hall plot was used to determine crystallite size D. In Williamson-Hall method plotting $\beta\cos(\theta)/\lambda$ as a function of $2\sin(\theta)/\lambda$ is used. The intercept of a linear extrapolation gives the particle size K/D, where constant K is 0.9 [11].

The morphology of layers was investigated with a scanning electron microscope (SEM) FEI Quanta 200F in secondary electron mode.

Optical characterization of thin films on glass substrate was made by UV-VIS spectrophotometer Spectronic GENESYS 8. Forbidden energy band gap E_g was determined from transmittance spectra's absorption edge using Tauc's relationship $(\alpha h\nu)^m = B(h\nu - E_g)$ and by extrapolating this dependency to $h\nu$ axis (light quantum energy) [12]. Absorption coefficient α (cm^{-1}) is calculated using transmittance coefficients of film on glass substrate and substrate without film. Coefficient m is used 1/2 for indirect transitions, 2 or sometimes 3/2 for direct transitions. Linear correlation analysis was made to choose the most suitable mode.

RESULTS AND DISCUSSION

The Scanning Electron Microscope images of as deposited and annealed CeO_2/Gd_2O_3 multilayer thin films cross-section are shown in Figures 1 and 2. It can be seen in Figures 1 and 2, that deposited layers are very dense and have columnar structure. When other authors [13] haven't found any clear changes for the morphology after annealing (900 °C), our experiment shows that surface became smoother after annealing sample in 650 °C temperature.

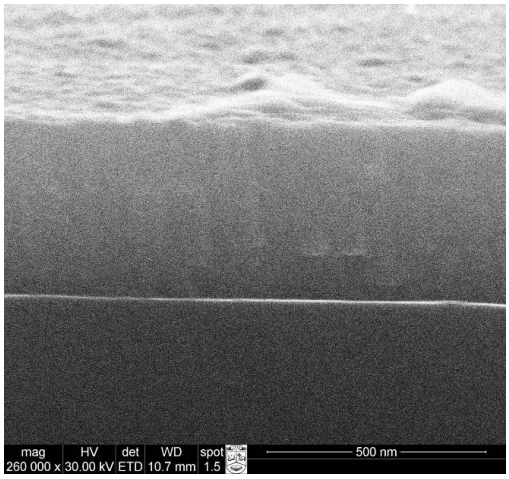

Fig. 1. SEM image of as deposited CeO_2/Gd_2O_3 multilayer film cross-section with magnification 260 000

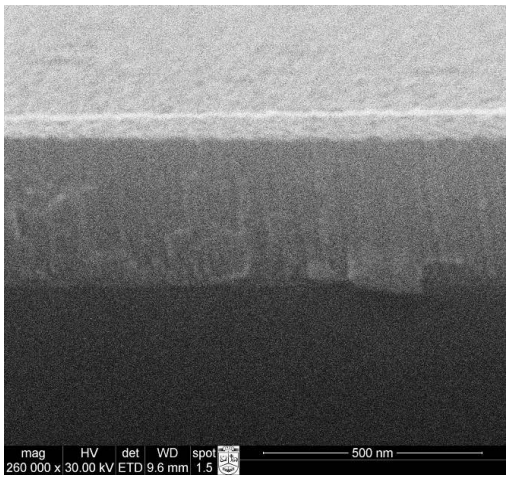

Fig. 2. SEM image of annealed (650 °C) CeO_2/Gd_2O_3 multilayer film cross-section with magnification 260 000

No evidences for multilayer structures were found. Secondary electron SEM images seen here have small sensitivity to Z-number contrast [14]. A big difference in electron work functions also is not expected for both lanthanide oxides. Breaking the sample was performed without cooling it in liquid nitrogen, but since Young's modulus isn't very different for CeO_2 ($E = 165$ GPa) [15] and Gd_2O_3 (148 GPa [16]), no reason for contrast due to different crack relief in multilayer film can be expected.

Averaged result of the measurements of layer thicknesses from SEM images is 370 nm. The disagreement of this result with prediction based on precise weighting results can be addressed to error caused by sample tilting effect. Also the weighting method has an error due to unknown exact density of the material, which may vary for different deposition methods and disagree with bulk material density that was used for calculations in this work.

Figure 3 shows the results of XRD analysis of as deposited and annealed multilayer films produced on the Si substrate. The diffraction peaks indicate that before annealing multilayer consists mainly of (111) textured CeO_2 (PDF Card No. 01-081-0792). Minor peaks of (200) and (220) orientation are also observed, what is typical for magnetron deposited thin films [2]. Gd_2O_3 peaks were not observed.

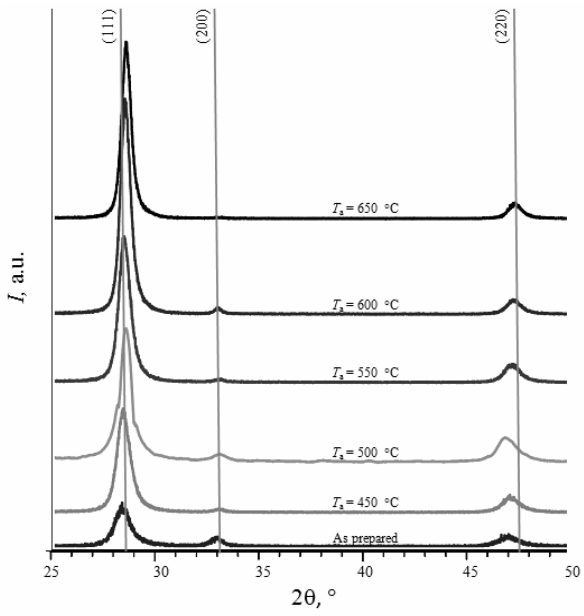

Fig. 3. XRD pattern of as deposited and annealed CeO_2/Gd_2O_3 multilayer films produced on the Si substrate

While the (220) peak of samples annealed in temperatures from 450 °C to 550 °C in obtained XRD pattern are shifted to smaller 2θ angle side, peak of the samples annealed in the 600 °C and 650 °C fits the $Gd_{0.1}Ce_{0.90}O_{1.95}$ etalon (PDF Card No. 01-075-0161) position. Since deposition was made by reactive sputtering, formation of non-stoichiometric ceria and (220) peak overlapping with triclinic $Ce_{11}O_{20}$ (222) peak (PDF Card No. 01-089-8435) is expected. The biggest shifting and asymmetry can be seen at (220) peak of the sample annealed in 500 °C temperature. Also the asymmetry of the peaks could indicate that some part of the layers could be mixed already during the deposition. Since strong ion-mixing process isn't expected during unbalanced magnetron deposition the reasons for enhanced Gd diffusion during the deposition of film on room temperature substrates can be radiation enhanced diffusion. Since the argon ion bombardment during deposition creates vacancies, diffusion coefficient can increase several times. Also bombardment of ions and electrons could heat the upper sample layers to temperatures up to 200 °C and more, what also can enhance diffusion. The third reason for enhanced diffusion is thermal stresses, caused by mismatch of linear thermal expansion coefficients of CeO_2 and Gd_2O_3 ($\alpha_{CeO_2} : \alpha_{Gd_2O_3} = 12.58\times10^{-6} : 7.57\times10^{-6}$). Linear thermal expansion coefficients of the film and substrate for 0 °C – 500 °C temperatures range are also different, $\alpha_{GDC10} = (9-12)\ 10^{-6}\ K^{-1}$ and $\alpha_{Si} \cong 4\cdot10^{-6}\ K^{-1}$ [17, 18], so XRD peak shifting due to stresses related to α mismatch can be expected. So a non-monotonous (220) peak shifting that can be seen in Fig. 4 can be caused either by stress relaxation or diffusion process induced layer mixing.

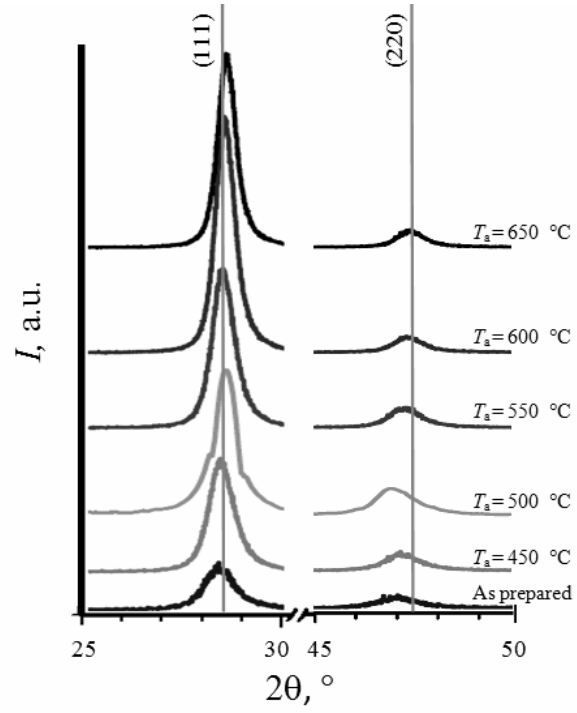

Fig. 4. XRD pattern of (111) and (220) peaks evolution upon annealing in air atmosphere

Crystallite size was calculated using Scherrer equation. After annealing (111) orientation crystallites increased from 6 nm to 8 nm and (220) orientation crystallites increased from 8 nm to 11 nm. Since the broadening of peaks could be attributed not only to crystallite size, but also to microstresses, Williamson-Hall plot was made to distinguish between these factors. The crystallite sizes obtained with both methods are compared in Fig. 5. According these results average crystallite size increased upon annealing from 4 nm to 5 nm. These results also mean that long columns that can be seen in SEM images are not contiguous, but consist of many crystallites.

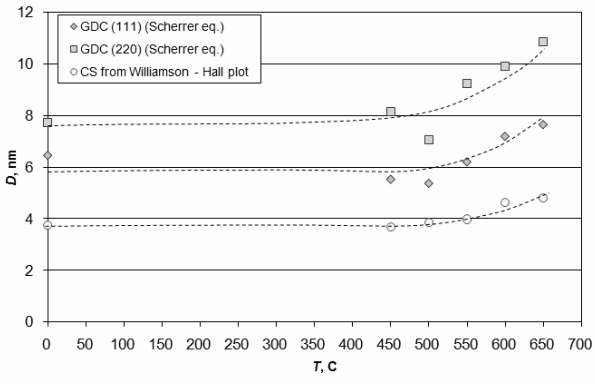

Fig. 5. Crystallite size of CeO_2/Gd_2O_3 multilayer thin films samples annealed in air atmosphere in temperatures from 450 °C to 650 °C

The results of optical transmittance measurement of CeO_2, Gd_2O_3 and multilayer CeO_2/Gd_2O_3 thin films deposited on glass substrate are shown in Fig. 6. In the CeO_2 spectrum we can see characteristic absorption edge at 350 nm which shifts to 340 nm after doping CeO_2 with larger band gap having Gd_2O_3. It can be seen that average transmittance in part of visible light wavelength range (600 nm – 760 nm) is slightly larger for GDC10 comparing to CeO_2 (69.5 % and 68.9 % respectively), what could be attributed to improved crystallinity after annealing.

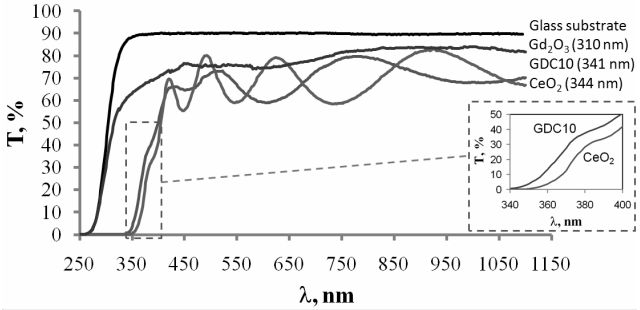

Fig. 6. Transmittance of CeO_2, Gd_2O_3 films and CeO_2/Gd_2O_3 multilayer film annealed in 500 °C temperature. Thicknesses of the films are indicated in the graph

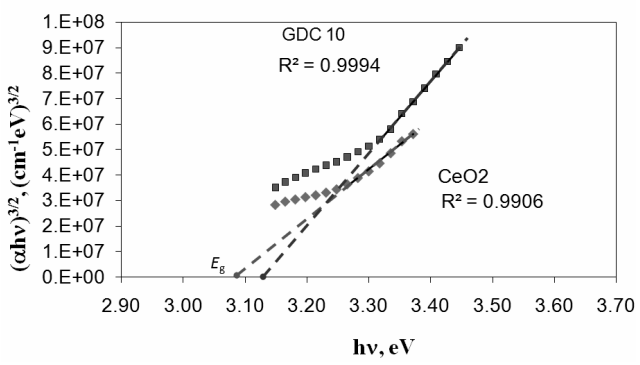

Fig. 7. Tauc's plot for CeO_2 and annealed CeO_2/Gd_2O_3 (GDC10) multilayer films produced on the glass substrates

Band gap of CeO_2 and annealed CeO_2/Gd_2O_3 multilayer films was determined from transmittance spectra's absorption edge using Tauc's relationship for direct electron transitions from valence to conduction band. Calculated band gap for CeO_2/Gd_2O_3 multilayer film annealed in 500 °C is $E_{g,GDC10} = 3.13$ eV. It is slightly larger than the calculated band gap of CeO_2 $E_{g,CeO_2} = 3.08$ eV. Band gap calculation results are smaller than those obtained for bulk material (~5 eV, [19]), but well agree with other authors results obtained for nanocrystalline pure and doped CeO_2 thin films (3.0 eV – 3.2 eV) [20]. The decrease of fundamental band gap is mainly deduced by quantum-size effect when the nanoparticle size is between 0 nm and 3 nm [11]. In this experiment, the crystallite size is in the range of 4 nm – 5 nm, so changes of the band gap width rather could be caused by existence of Ce^{3+} ions, oxygen vacancies and various types of defects that may be the reason of bandgap narrowing due to so called band tailing, what means that the band edges at E_v (valence band top energy) and E_c (energy of the bottom of conduction band) are no longer well defined cut-off energies and there are electronic states above E_v and below E_c, where the density of states falls sharply with energy away from the band edges [12].

CONCLUSIONS

SEM and XRD results showed that Gd doped ceria thin films can be obtained by solid state reaction of CeO_2/Gd_2O_3 multilayer films deposited by direct current magnetron sputtering and annealing them for 1h in 600 °C and higher temperature. SEM cross-section images showed surface smoothing after 650 °C temperature annealing. The crystallite size determination shows that long columns of film that can be seen in SEM images are not contiguous, but consist of many crystallites. Optical transmittance measurement and band gap determination showed band gap shifting what can be attributed to changes in electronic structure of material.

Acknowledgements

The authors thank M. Lelys from Lithuanian Energy Institute for performing the XRD measurements and also T. Tamulevičius from Kaunas University of Technology for SEM imaging.

REFERENCES

1. **Kharton, V. V., Marques, F. M. B., Atkinson, A.** Transport Properties of Solid Oxide Electrolyte Ceramics: a Brief Review *Solid State Ionics* 174 (1 – 4) 29 October 2004: pp. 135 – 149.
2. **Briois, P., Billard, A.** A Comparison of Electrical Properties of Sputter-deposited Electrolyte Coatings Dedicated to Intermediate Temperature Solid Oxide Fuel Cells *Surface and Coatings Technology* 201 (3 – 4) 5 October 2006: pp. 1328 – 1334.
3. **Zhen, Y. D., et al.** Fabrication and Performance of Gadolinia-doped Ceria-based Intermediate-temperature Solid Oxide Fuel Cells *Journal of Power Source* 178 (1) 15 March 2008: pp. 69 – 74.
4. **Laukaitis, G., Dudonis, J.** Microstructure of Gadolinium Doped Ceria Oxide Thin Films Formed by Electron Beam Deposition *Journal of Alloys and Compounds* 459 2008: pp. 320 – 327.
5. **Pryds, N., Rodrigo, K., Linderoth, S., Schou, J.** The Growth of Gadolinia-doped Ceria by Pulsed Laser Deposition *Applied Surface Science* 255 2009: pp. 5232 – 5235.
6. **Song, H. Z., et al.** Aerosol-assisted MOCVD Growth of Gd2O3-doped CeO2 Thin SOFC Electrolyte Film on Anode Substrate *Solid State Ionics* 156 2003: pp. 249 – 254.
7. **Musila, J., Baroch, P., Vlcek, J., Nam, K. H., Han, J. G.** Reactive Magnetron Sputtering of Thin Films: Present Status and Trends *Thin Solid Films* 475 2005: pp. 208 – 218.
8. **Leng, Y. J., Chan, S. H., Jiang, S. P., Khor, K. A.** Low-temperature SOFC with Thin Film GDC Electrolyte Prepared In Situ by Solid-state Reaction *Solid State Ionics* 170 (1 – 2) 14 May 2004: pp. 9 – 15.

9. **Kelly, P. J., Arnell, R. D.** Magnetron Sputtering: a Review of Recent Developments and Applications *Vacuum* 56 2000: pp. 159 – 172.
10. **Steele, B. C. H.** Appraisal of $Ce_{1-y}Gd_yO_{2-y/2}$ Electrolytes for IT-SOFC Operation at 500 °C *Solid State Ionics* 129 (1 – 4) April 2000: pp. 95 – 110.
11. **Vives, E. Gaffet, C. Meunier** X-ray Diffraction Line Profile Analysis of Iron Ball Milled Powders *Materials Science and Engineering A* 366 2004: pp. 229 – 238.
12. **Safa Kasap, Peter Capper** (Eds.) Handbook of Electronic and Photonic Materials. Springer, 2006: pp. 57 – 62.
13. **Chen, M. Y., et al.** Effects of Ion Irradiation and Annealing on Optical and Structural Properties of CeO_2 Films on Sapphire *Physica B* 389 2007: pp. 263 – 268.
14. **Brundle, C. R., Evans, Ch. A., Wilson, Sh.** (Editors) Encyclopedia of Materials Characterization – Surfaces, Interfaces, Thin Films. Butterworth-Heinemann, 1992: p. 73.
15. **Mogensen, M., Sammes, N. M., Tompsett, G. A.** Physical, Chemical and Electrochemical Properties of Pure and Doped Ceria *Solid State Ionics* 129 2000: pp. 63 – 94.
16. **Haglund, J. A., Hunter, O.** Elastic Properties of Polycrystalline Monoclinic Gd2O3 *Journal of the American Ceramic Society* 56 (96) 1973: pp. 327 – 330.
17. **Hayashi, H., et al.** Thermal Expansion of Gd-doped Ceria and Reduced Ceria *Solid State Ionics* 132 2000: pp. 227 – 233.
18. **Mazur, A. V., Gasik, M. M.** Thermal Expansion of Silicon at Temperatures up to 1100 °C *Journal of Materials Processing Technology* 209 2009: pp. 723 – 727.
19. **Huff, H. R., Gilmer, D. C.** High Dielectric Constant Materials – VLSI MOSFET Applications. Springer. 2005: 710 p.
20. **Hartridge, A., et al.** Optical Constants of Nanocrystalline Lanthanide-doped Ceria Thin Films with the Fluorite Structure *Journal of Physics and Chemistry of Solids* 59 (6 – 7) 1998: pp. 859 – 866.

Presented at the National Conference "Materials Engineering'2009" (*Kaunas, Lithuania, November 20, 2009*)

DOI: 10.5755/j02.ms.26046